Acta Cryst. (1957). **10**, 281

The Structure of High-Temperature Potassium Chlorate

By G. N. Ramachandran and M. A. Lonappan

Department of Physics, University of Madras, Madras 25, India

(*Received* 26 *July* 1956 *and in revised form* 29 *October* 1956)

Potassium chlorate (monoclinic, $2/m$) undergoes a structural transformation at 250° C., changing to an orthorhombic form above this temperature. The structure of the high-temperature modification has been deduced from powder photographs obtained above 250° C. The X-ray pattern corresponds closely to that of the low-temperature form, but contains a few extra lines which can be indexed only on the basis of a unit cell twice that of low-$KClO_3$. Utilizing the observation on twinning and other physical properties, the structure of high-$KClO_3$ has been worked out. It may be considered to be a mixture of the structure of the two twins of low-$KClO_3$, the alternation occurring twice per unit cell along the c axis. The atomic arrangement and coordination is similar to that found in low-$KClO_3$. The calculated structure factors agree well with the observed intensities.

The principal thermal expansion coefficients have been determined for the temperature range 280–325° C. These are also in accord with the proposed structure.

1. Introduction

Madan (1886) observed that if potassium chlorate in the form of plates parallel to the c planes is heated above 250° C. and then cooled, the plates exhibited a peculiar pearly lustre. On heating again above this temperature, the crystals became transparent and the phenomenon was reversible. The transition temperature was estimated by Madan to occur between 245 and 248° C. Careful measurements made in this laboratory gave a temperature of 250±1° C. Lord Rayleigh (1888, 1889) explained the pearly lustre as arising from the occurrence of multiple twins in the crystal plate. Potassium chlorate is monoclinic (b axis unique), so that if the crystals are twinned on the c plane and the twins occur alternately as thin flakes in large numbers in the thickness of the crystal, then the large number of multiple reflexions occurring at the planes of separation would lead to the pearly lustre of the crystal. Lord Rayleigh also remarked that the iridescent colour exhibited by some crystals obtained from solution (Stokes, 1885) is also due to the same cause; only in this case all the lamellae are exactly of the same thickness, of the order of a micron. It is also found that on heating above 250° C. the iridescence disappears, and on cooling only the pearly lustre is obtained.

Several studies have been made on the optical behaviour of potassium chlorate, particularly in relation to its iridescence (Wood, 1906; Ramdas, 1926; Raman & Krishnamurthy, 1953). The structure of potassium chlorate at room temperature was determined by Zachariasen (1929), who found that all the atoms in a molecule of $KClO_3$, except one oxygen atom, occur very nearly in a plane perpendicular to the c plane (Fig. 3(a)). Thus the c plane is a pseudo-plane of symmetry (pseudo-glide plane) and this explains why the crystal forms multiple twins so readily. The structure of the twin will be continuous across the twin plane, except for the position of one oxygen per molecule.

2. Effect of transition on crystal properties

The X-ray study of Sirkar (1930) clearly showed that the pearly crystals of $KClO_3$ are in fact multiply twinned. This has been confirmed by the authors by taking the Laue pattern of a pearly crystal with the X-ray beam normal to the surface, although Sirkar's indexing of the spots was found to be in error. The effect of twinning is to produce a doubling of the spots in this Laue pattern (Fig. 1). The iridescent crystals also exhibit the same X-ray pattern as the pearly crystals at room temperature. It was observed by one of the authors (G. N. R.) some time ago (during some preliminary experiments made at Bangalore in 1944) that on heating above 250° C., the doubling of the spots disappears in both pearly as well as iridescent crystals and that the single set of spots is then arranged symmetrically both about the horizontal and vertical lines. This indicates that there is no twinning above this temperature and that the symmetry becomes orthorhombic.

The thermal expansion of potassium chlorate has been recently determined up to 200° C. (Lonappan, 1955). The lattice constants of the crystal at different temperatures may be calculated from these results and are given in Table 1. The cell constants at 20° C. were obtained from the data of Zachariasen (1929). If the lattice is rectangular, then the relation $c\cos\beta = \frac{1}{2}a$ must be satisfied. The data in the last two columns of the table show that the equality in fact holds at about 120° C., but that $\cos\beta$ progressively deviates from $\frac{1}{2}a$ at higher temperatures. Thus, the lattice of the low-temperature modification of $KClO_3$ is def-

Table 1. *Lattice dimensions of* $KClO_3$ *at various temperatures*

Temperature (°C.)	a (Å)	b (Å)	c (Å)	β (°)	$c \cos \beta$ (Å)	$\frac{1}{2}a$ (Å)	$c \cos \beta - \frac{1}{2}a$ (Å)
20	4·647	5·585	7·085	109·63	2·381	2·324	0·057
90	4·665	5·600	7·122	109·25	2·348	2·333	0·015
150	4·679	5·611	7·152	108·93	2·321	2·340	−0·019
200	4·692	5·621	7·180	108·61	2·292	2·346	−0·054
250	4·706	5·632	7·209	108·29	2·262	2·353	−0·091

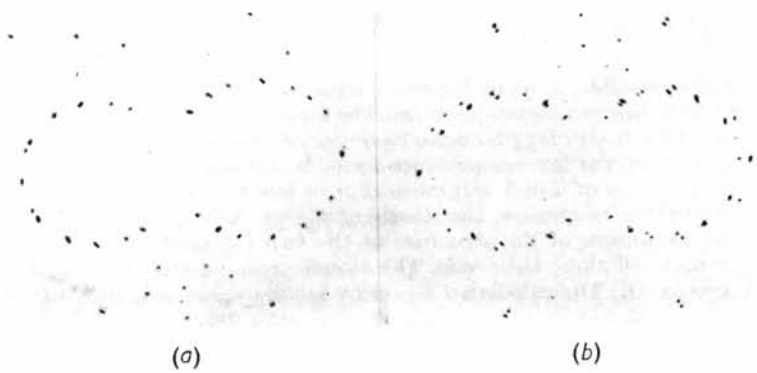

(*a*) (*b*)

Fig. 1. Laue patterns obtained with X-ray beam normal to the c planes with (*a*) untwinned crystal, (*b*) multiply twinned crystal which had been heated above 250° C. and then cooled.

initely not orthorhombic (rectangular) at 250° C., and the transition therefore must be abrupt. This is also to be expected from the structure of the low-temperature form, in which the plane of the O_3 group is at an angle of 34° to the normal to the c planes. This is also confirmed by the thermal expansion data, which give a value of 30° (Lonappan, 1955). This inclination continues to be nearly the same up to 200° C. The point is that there is no evidence to indicate that the O_3 planes slowly tilt with increase of temperature so that at the transition point the structure takes up a higher symmetry.

Infra-red (Ramdas, 1952) and Raman-effect (Shantakumari, 1950) studies show that the chlorate ion has practically trigonal symmetry in the crystal also. The frequencies are practically the same as those of the free ion in solution and the influence of the potassium ion on the vibration of the chlorate ion is small in the crystalline state. Shantakumari (1950) finds in addition that no abrupt changes occur either in the intensity or frequency of the Raman lines at 250° C. We may deduce from this that the neighbourhood of the O_3 groups is not appreciably affected by the transition occurring at this temperature.

To summarize, the previous observations suggest that the structure becomes orthorhombic above the transition temperature, that the high-temperature modification is not appreciably different from the low-temperature form, and that the former should be such that it could change over with equal ease into either twin of the latter. By means of an X-ray study above 250° C., it has been possible to determine the structure of the high-temperature modification, which satisfies these requirements.

3. Experimental details

It was not found possible to mount single crystals and heat them above the transition temperature without their breaking up. Rotation photographs could not therefore be obtained of the high-temperature modification. Only powder photographs were taken, using powdered $KClO_3$ kept in a thin silica tube. A number of pictures were taken using the Unicam high-temperature camera at different temperatures both above and below the transition point, namely at 30, 100, 150, 200, 250, 280, 300 and 325° C. A comparison of the photographs obtained at 200° C. (well below the transition temperature) and at 280° C. (well above it) revealed some significant differences, which are discussed below. The photographs obtained at 280° C. and 325° C. were used for determining the thermal expansion of potassium chlorate in this range of temperature. Those obtained at temperatures below 250° C. were utilized for checking the thermal expansion data obtained by the single-crystal method (Lonappan, 1955) up to 200° C.

4. Unit cell of the high-temperature modification

All the photographs taken above the transition temperature contained a few extra lines, not found below this temperature. The photographs taken at 250° C. showed these lines faintly, probably because the temperature was not quite steady and was partly above and partly below the transition point. Notable among the extra lines were those at $\sin^2 \theta = 0{\cdot}039$ and $\sin^2 \theta = 0{\cdot}045$. If one assumes as an approximation that the unit cell is the same as that at 200° C., then

most of the lines observed at 280° C. correspond to integral indices, except the extra lines, which correspond to half-integral values for l. (The indices with respect to the low-temperature unit cell are given in column 4 of Table 2.)

Table 2. *Test of orthorhombic cell at* 280° C.

The values of $\sin^2\theta$ were calculated assuming $a = 4{\cdot}74$, $b = 5{\cdot}64$, $c = 13{\cdot}80$ Å, $\lambda = 1{\cdot}542$ Å

hkl (new cell)	$(\sin^2\theta)_c$	$(\sin^2\theta)_o$	$h_0k_0l_0$ (old cell)
101	0·0296	0·0297	$100, 10\bar{1}$
012	0·0312	0·0312	011
102	0·0390	0·0391	$10\frac{1}{2}, 10\frac{\bar{3}}{2}$
110	0·0452	0·0455	$11\frac{\bar{1}}{2}$
013	0·0468		$01\frac{3}{2}$
111	0·0483	0·0483	$110, 11\bar{1}$
004	0·0499	0·0503	002
112	0·0577	0·0580	$11\frac{1}{2}, 11\frac{\bar{3}}{2}$
014	0·0686	0·0688	012
113	0·0733	0·0737	$111, 11\bar{2}$
020	0·0747	0·0745	020
022	0·0872	0·0869	021
200	0·1060	0·1059	$20\bar{1}$
105	0·1045		$102, 10\bar{3}$
121	0·1043		$120, 12\bar{1}$
202	0·1185	0·1180	$200, 20\bar{2}$
024	0·1246	0·1242	022
115	0·1232		$112, 11\bar{3}$
123	0·1293	0·1295	$121, 12\bar{2}$
204	0·1559	0·1565	$201, 20\bar{3}$
125	0·1792	0·1800	$122, 12\bar{3}$
131	0·1976	0·1978	$130, 13\bar{1}$
034	0·2179	0·2175	032
224	0·2306	0·2301	$221, 22\bar{3}$
311	0·2603	0·2608	$312, 31\bar{1}$
232	0·2865	0·2866	230
040	0·2987	0·2989	040

It was found that all the observed lines at 280° C. could be accounted for on the basis of the following orthorhombic unit cell:

$$a = 4{\cdot}74, \quad b = 5{\cdot}64, \quad c = 13{\cdot}80 \text{ Å}.$$

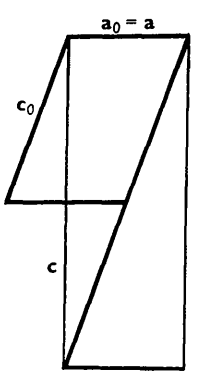

Fig. 2. Relation between the monoclinic ($\mathbf{a}_0, \mathbf{b}_0, \mathbf{c}_0$) and pseudo-orthorhombic ($\mathbf{a}, \mathbf{b}, \mathbf{c}$) unit cells of low-$KClO_3$. When the symmetry is truly orthorhombic, as in high-$KClO_3$, we have $a_0 = 2c_0 \cos\beta$.

These dimensions of the unit cell were arrived at by a method of trial and error, and the agreement of the calculated spacings with those observed is shown in Table 2. The extra lines observed above the transition temperature are shown in this table in italics. It will be noticed that the a and b axes of the new cell are nearly the same as below 250° C. (Table 1), but that the new c is nearly equal to $2c \sin\beta$ of the old cell.

The relationship between the old and new cells is shown in Fig. 2. The axes of the low-temperature unit cell are marked $\mathbf{a}_0$ and $\mathbf{c}_0$ and are indicated by thick lines. The two sets of axes are related as follows:

$$\mathbf{a} = \mathbf{a}_0, \quad \mathbf{b} = \mathbf{b}_0, \quad \mathbf{c} = 2\mathbf{c}_0 + \mathbf{a}_0$$

Denoting the old indices by $h_0k_0l_0$ and the new by hkl, the relation between them is given by

$$h = h_0, \quad k = k_0, \quad l = 2l_0 + h_0$$

and

$$h_0 = h, \quad k_0 = k, \quad l_0 = \tfrac{1}{2}(l-h).$$

If l_0 is to be integral (as is the case for the unit cell below the transition point), then $(l-h)$ should be even, which is the same as saying that $h+l$ is even. Thus the extra lines found above 250° C. will all have $(h+l)$ odd.

5. Space group and structure of high-$KClO_3$

The structure determined by Zachariasen (1929) for low-$KClO_3$ is shown in Fig. 3(*a*) (we shall use the terms low-$KClO_3$ and high-$KClO_3$ to denote the room-temperature modification and the one above 250° C.). The thick lines indicate the projected unit cell and the thin lines mark out the derived near-rectangular unit cell of twice the area. If the relation $c_0 \cos\beta = \frac{1}{2}a_0$ is exactly satisfied, then the latter would be truly rectangular. This is not so, and further the structure has no reflexion or glide planes parallel to (001). Consequently, in low-$KClO_3$, there will in general be pairs of lattice planes like $(h_0k_0l_0)$ and (h_0,k_0,h_0+l_0) whose spacings are very nearly equal but whose structure factors may be quite different, e.g. $F(100) = 7{\cdot}1$, while $F(10\bar{1}) = 17{\cdot}0$ (Zachariasen, 1929). In high-$KClO_3$ such a pair must have the same spacing and the same structure factor. Now, it is found that the relative intensities of the various lines in the powder photograph are practically unchanged as the crystal passes through the transition point. In the powder photograph of low-$KClO_3$, the pair of reflexions $h_0k_0l_0$ and h_0,k_0,h_0+l_0 always superpose, and both correspond to the same reflexion in the high-temperature modification. Thus it follows that the structure of high-$KClO_3$ must be such that the intensity of a reflexion given by it must be nearly equal to the average of the intensities of the pair of reflexions in low-$KClO_3$ to which it corresponds. This is equivalent to saying that the intensity of reflexion given by a lattice plane of high-$KClO_3$ is nearly the same as the

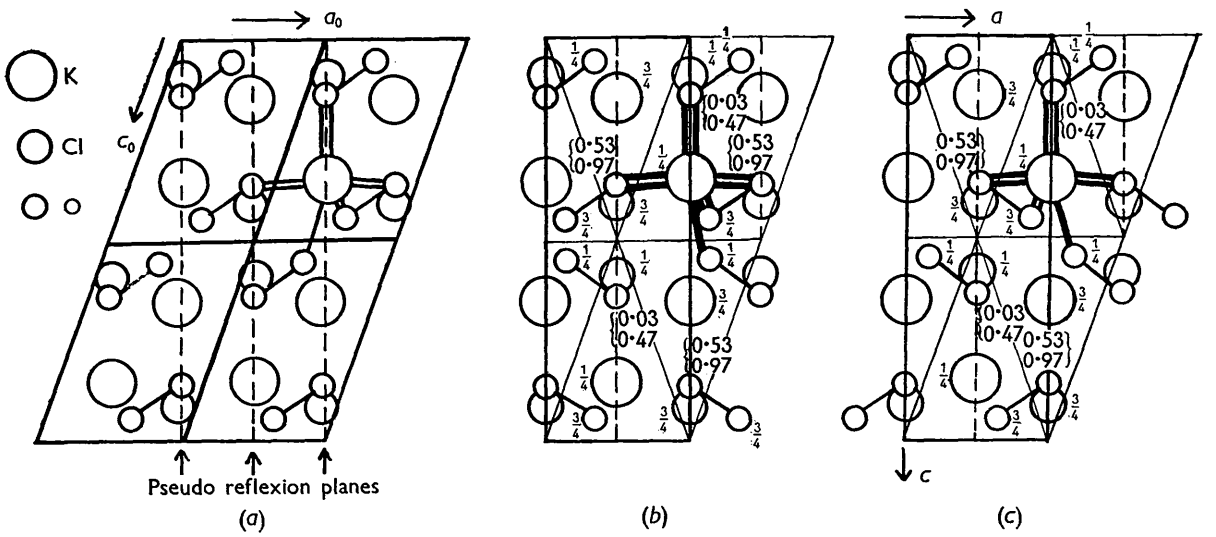

Fig. 3. (*a*) Atomic arrangement in low-$KClO_3$. Four unit cells are shown. (*b*) Possible atomic arrangement in high-$KClO_3$, corresponding to the space group *Pcmb*. This differs from (*a*) only in the positions of two oxygen atoms. (*c*) Atomic arrangement in high-$KClO_3$ corresponding to the space group *Pcmn*. This also differs from (*a*) only in the positions of two oxygen atoms per unit cell. This is the structure favoured for high-$KClO_3$.

average of the intensities of the same reflexion given by the two twins of low-$KClO_3$.

Such a result would be closely approximated if the structure of high-$KClO_3$ is itself a mixture in some way of equal proportions of the two twin structures of low-$KClO_3$. The fact that the unit cell of high-$KClO_3$ has twice the extension normal to the *c* planes as that of low-$KClO_3$ lends further support to this idea. Then half the cell along the *c* axis may correspond to the structure of one twin, while the other half may correspond to the other twin.

Two structures appear to be possible, if they are to satisfy the above considerations. They are shown in Figs. 3(*b*) and 3(*c*). If they are compared with Fig. 3(*a*) (structure of low-$KClO_3$), it will be seen that both of them differ from the latter in the following respects. The K, Cl and two of the three O atoms in a molecule of $KClO_3$ are practically the same as in low-$KClO_3$. Of the remaining four oxygens per unit cell (one for each molecule of $KClO_3$), two have changed their positions from those in low-$KClO_3$ to symmetric positions obtained by reflexion in the *a*(100) plane. Thus, two of the four O_3 groups in the unit cell have the same orientation as in Fig. 3(*a*), while the other two have an orientation obtained by reflexion in the *a* plane (namely, corresponding to the twin of the structure shown in Fig. 3(*a*)).

Although they both have the above property, the two structures shown in Figs. 3(*b*) and 3(*c*) are not identical. A careful examination shows that these are the only two structures which can be derived from the original one (i.e. low-$KClO_3$) by combining it with its twin structure so that the resultant structure has orthorhombic symmetry. The symmetry elements of the two structures are shown respectively in Figs. 4(*a*) and 4(*b*). It will be noticed that the space groups are different, the former being D_{2h}^{11}–*Pcmb* and the latter D_{2h}^{16}–*Pcmn*.

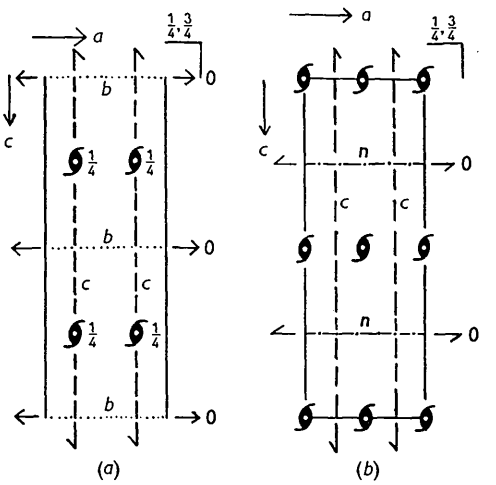

Fig. 4. Symmetry elements (*a*) of structure shown in Fig. 3(*b*) (space group *Pcmb*), (*b*) of structure shown in Fig. 3(*c*) (space group *Pcmn*).

The choice between the two structures could be made on the basis of the observed new lines in the powder diagram above 250° C. The first two of these are*

hkl	$(\sin^2\theta)_{calc.}$	$(\sin^2\theta)_{obs.}$
102	0·0391	0·039
110	0·0452	0·045
013	0·0468	

* Hereafter all indices will be with reference to the orthorhombic unit cell of high-$KClO_3$.

Considering the structure (Fig. 3(*b*)) with space group D_{2h}^{11}–*Pcmb* we see that 102 is an allowed reflexion for this structure, but that *both* 110 and 013 are forbidden. In other words, no line should be observed at about $\sin^2\theta = 0{\cdot}045-0{\cdot}047$. Since there is a line at $\sin^2\theta = 0{\cdot}045$, which is in fact stronger than the line at $\sin^2\theta = 0{\cdot}039$, this structure must be ruled out.

Considering the other structure (Fig. 3(*c*)) with space group D_{2h}^{16}–*Pcmn* we see that 013 is still forbidden, but that both 102 and 110 are allowed, and both the newly observed lines are explained by this structure. As will be shown below, the calculated structure factors are also in good agreement with observation.

6. Detailed examination of the new structure

Further confirmation regarding the structure of high-$KClO_3$ was obtained by calculating the structure factors for some of the reflexions. The following coordinates were assumed for the atoms, which lead to practically the same distances between the various atoms as in low-$KClO_3$:

Space group: *Pcmn*; $Z = 4$.

4 K, 4 Cl, 4 O at positions 4(*c*):

$u, \frac{1}{4}, w;\ \bar{u}, -\frac{1}{4}, \bar{w};\ \frac{1}{2}+u, -\frac{1}{4}, \frac{1}{2}-w;\ \frac{1}{2}-u, \frac{1}{4}, \frac{1}{2}+w,$

with

$u_K = 0{\cdot}50$ (2·37 Å), $w_K = -0{\cdot}135$ (−1·86 Å),
$u_{Cl} = 0{\cdot}00$ (0·00 Å), $w_{Cl} = 0{\cdot}085$ (1·17 Å),
$u_O = 0{\cdot}345$ (1·64 Å), $w_O = 0{\cdot}055$ (0·76 Å).

8 O′ at positions 8(*d*):

$x, y, z;\ \frac{1}{2}-x, \frac{1}{2}-y, \frac{1}{2}+z;\ \bar{x}, \frac{1}{2}+y, \bar{z};\ \frac{1}{2}+x, \bar{y}, \frac{1}{2}-z;$
$\bar{x}, \bar{y}, \bar{z};\ \frac{1}{2}+x, \frac{1}{2}+y, \frac{1}{2}-z;\ x, \frac{1}{2}-y, z;\ \frac{1}{2}-x, y, \frac{1}{2}+z,$

with

$x=0{\cdot}00$ (0·00 Å), $y=0{\cdot}47$ (2·65 Å), $z=0{\cdot}14$ (1·93 Å).

The above coordinates were obtained by comparing the structure with that of low-$KClO_3$, as determined by Zachariasen (1929) and making the interatomic distances nearly the same in both forms. Zachariasen's structure leads to widely different values for the three Cl–O distances, namely 1·42, 1·42 and 1·60 Å, which are most probably not correct. The structure assumed for high-$KClO_3$ has also the same feature; the three values are 1·45, 1·45 and 1·69 Å, where again the differences are not significant. However, since Zachariasen's data are the only ones available for low-$KClO_3$, they were utilized for the present study. No significance is to be attached to the exact values of the atomic coordinates reported here. Rather the attempt has been to work out the general scheme of atomic arrangement in the high-temperature form and not the exact location of the atoms.

The calculated structure factors and intensities for all the possible powder lines up to $\sin^2\theta = 0{\cdot}100$ are given in Table 3.

Table 3. *Observed and calculated intensities of powder lines of high-*$KClO_3$

Indices	$\sin^2\theta$	F	$\lvert F\rvert^2$	$I_c\times10^{-3}$§	I_o‖
002	0·0125	36·1	1303	403·1	*
101	0·0296	33·7	1135	283·9	4†
012	0·0312	−18·9	357	82·5	2†
102	0·0390	−15·3	234	42·3	2
110	0·0452	−23·2	538	82·2	4
111	0·0483	−75·4	5683	1614·8	10
004	0·0499	−131·5	17292	1184·5	7
103	0·0546	− 7·5	56	6·9	—
112	0·0577	−16·6	276	63·8	4‡
014	0·0686	−79·8	6368	596·7	6
113	0·0733	−72·9	5214	921·5	8
020	0·0747	−84·1	7093	297·7	2
104	0·0764	−19·5	380	31·1	—
022	0·0872	−42·4	1798	124·9	1
114	0·0951	− 3·4	12	1·5	—
121	0·1043	31·7	1005	111·7	6
105	0·1045	−27·8	773	42·4	
200	0·1060	132·0	17424	471·6	

* Beyond range of camera.
† Visually estimated intensity affected by heavy background.
‡ Superposed on a spurious line from the backstop. The spurious line persists at lower temperatures also.
§ Assuming temperature factor $B = 4$ Å^2.
‖ Visual estimates, on an arbitrary scale.

It turns out that only four oxygen atoms (O) contribute to the structure factor if $(h+l)$ is odd, i.e. for the extra lines occurring above 250° C. which are forbidden for low-$KClO_3$. For the other reflexions, all atoms contribute. The indices of the extra lines (those with $h+l$ odd) are printed in italics. It will be seen that the calculated intensities are in reasonable agreement with observation.

7. Configuration of atoms in high-$KClO_3$

Each potassium atom is surrounded by 9 oxygen atoms. The K–O distances, compared with those in low-$KClO_3$, are given in Table 4. The similarity of the

Table 4. K–O *distances for low- and high-*$KClO_3$.
The number of bonds of each type are indicated within brackets

Type of bond	Distance in low-$KClO_3$ (Å)	Distance in high-$KClO_3$ (Å)
K–O′	2·73(2), 3·09(2), 2·86(2)	2·85(2), 3·35(2), 2·85(2)
K–O	2·84(1), 3·12(2)	2·72(1), 3·11(2)
Average	2·94	3·00

K–O coordination in the two structures may also be seen by comparing Figs. 3(*a*) and 3(*c*). The nine K–O bonds from a particular potassium atom are marked by thin lines in Fig. 3; where the atom is bonded to two oxygens vertically above and below, a double bond is shown. It will be noticed that the configuration of bonds in the proposed structure of high-$KClO_3$ is the same as in low-$KClO_3$. In the rejected structure

for high-$KClO_3$, on the other hand, the bonds are seen to be of a different type and also not quite symmetric.

The structure is therefore perfectly reasonable from the crystallochemical point of view. The coordinates could be refined, but it was not thought worth while to do this with only the powder data.

It is also obvious that at the boundary between two twins of low-$KClO_3$, a coordination very similar to that which obtains in high-$KClO_3$ would occur. Thus, the very ready formation of twins is explained. In fact, high-$KClO_3$ may be considered as low-$KClO_3$ twinned on c planes spaced at intervals of $\frac{1}{2}c$. On cooling below the transition point the interval becomes large, of the order of a few microns, and the individual twins then have only monoclinic symmetry.

8. Thermal expansion of high-$KClO_3$

A further confirmation of the main features of the structure was obtained from a study of the thermal expansion of $KClO_3$ above 250° C. The two powder photographs obtained at 280 and 325° C. were carefully measured and the thermal expansion coefficients (α) were determined from the variation in the θ values of the different lines. Nine of the sharper and more intense lines in the range $\theta = 10$–$24°$ were measured and the data are given in Table 5.

Table 5. *Measured and calculated values of thermal expansion coefficients of high-*$KClO_3$

Indices (new)	θ (°)	$\alpha \times 10^5$(/°C.) (measured)	$\alpha \times 10^5$(/°C.) (calculated)
110	12·34	3·2	5·2
111	12·74	2·1	6·4
004	13·00	20·3	23·3
014	15·28	18·8	16·1
113*	15·80	13·6	13·2
020*	15·89	−4·1	−3·1
200†	19·11	13·5	11·1
123	21·28	9·7	5·5
204	23·39	14·6	15·0

* Of the close doublet, the one having the lower value of θ was taken as 113, since this is confirmed by calculating $\sin^2\theta$ for both (see Table 2).

† The lines, 200, 105, 121 superpose, but only 200 is taken for the thermal expansion as its intensity is much higher than that of the other two (see Table 3).

Since the θ values were quite small, the accuracy of the individual measurements of thermal expansion was not expected to be high. However, two interesting facts were observed, namely that the 020 spacing showed a contraction and that the expansion coefficients varied widely for different directions, showing that the principal expansion coefficients are appreciably different from one another. Since the indices of these were well established (the table itself contains notes on those lines where there was a doubt), the principal coefficients (α_a, α_b, α_c) were determined by the method of least squares.

Nine equations could be obtained of the form

$$\alpha = \alpha_a \cos^2\varphi_a + \alpha_b \cos^2\varphi_b + \alpha_c \cos^2\varphi_c ,$$

where

$$\cos^2\varphi_a = h^2a^{*2}/[h^2a^{*2}+k^2b^{*2}+l^2c^{*2}]^{\frac{1}{2}} ,$$
$$\cos^2\varphi_b = k^2b^{*2}/[h^2a^{*2}+k^2b^{*2}+l^2c^{*2}]^{\frac{1}{2}} ,$$
$$\cos^2\varphi_c = l^2c^{*2}/[h^2a^{*2}+k^2b^{*2}+l^2c^{*2}]^{\frac{1}{2}} .$$

Three normal equations in α_a, α_b, α_c were obtained from these and were solved to obtain the principal expansions. These calculated values of α are also given in Table 5. The probable errors were calculated from the differences by the usual method. The final values were:

$$\alpha_a = 11{\cdot}1 \pm 2{\cdot}3 \times 10^{-5}/°\text{C.},\ \alpha_b = -3{\cdot}1 \pm 2{\cdot}7 \times 10^{-5}/°\text{C.},$$
$$\alpha_c = 23{\cdot}3 \pm 2{\cdot}5 \times 10^{-5}/°\text{C.}$$

As expected, the difference between the calculated and observed values are appreciable, but the general agreement between the two shows that there is no mistake about the trend of the data.

The thermal expansion data appear to be in good agreement with the structure. The O_3 groups in the structure are all oriented in two directions, the normal to the O_3 plane making an angle of about $\pm 35°$ with the c axis. The b axis is a direction common to all the O_3 planes (Fig. 3(c)). At these high temperatures, the tilting oscillations of the O_3 planes will have a large amplitude and therefore the expansion normal to the planes will be large. Further, it is likely that the crystal will contract in a perpendicular direction (cf. the behaviour of calcite). Since the b direction is common to both the O_3 planes, it is not surprising that the expansion coefficient in this direction is negative.

Further, in the ac plane, the normals to the two sets of O_3 planes are at an angle of $\pm 35°$ to the c axis. Consequently if we assume that α_n, α_p are the contribution to thermal expansion normal and parallel to the planes, then we have

$$\alpha_c = \alpha_n \cos^2 35° + \alpha_p \sin^2 35° ,$$
$$\alpha_a = \alpha_n \sin^2 35° + \alpha_p \cos^2 35° .$$

Substituting the value $-3{\cdot}1 \times 10^{-5}$ found along the b axis for α_p and putting in the values of α_c and α_a, we get from the above two equations $\alpha_n = 36{\cdot}5 \times 10^{-5}$ and $39{\cdot}5 \times 10^{-5}$ respectively. The mean value, namely 38×10^{-5}, may be taken as the expansion coefficient normal to the plane of the oxygen atoms.

Taking thus

$$\alpha_n = 38 \times 10^{-5} \quad \text{and} \quad \alpha_p = -3 \times 10^{-5} ,$$

we get

$$\alpha_c = 23{\cdot}7 \times 10^{-5}/°\text{C.}\ \ (23{\cdot}3 \pm 2{\cdot}5 \times 10^{-5}/°\text{C.})$$

and

$$\alpha_a = 10{\cdot}7 \times 10^{-5}/°\text{C.}\ \ (11{\cdot}1 \pm 2{\cdot}3 \times 10^{-5}/°\text{C.}) ,$$

which are in excellent agreement with the observed values indicated in brackets.

This discussion shows that the assumption of two sets of O_3 groups symmetrically disposed with respect

to the a plane, making angles of $\pm 35°$ with the c axis, is in good agreement with the thermal expansion data. This is considered to be a good supporting evidence for the structure proposed in § 6 for high-$KClO_3$.

One of us (M. A. L.) is grateful to the University of Madras for the award of a Research Studentship, which made this investigation possible.

References

LONAPPAN, M. A. (1955). *Proc. Phys. Soc.* B, **68**, 75.
MADAN, H. G. (1886). *Nature, Lond.* **34**, 66.
RAMAN, C. V. & KRISHNAMURTHY, D. (1953). *Proc. Indian Acad. Sci.* A, **36**, 315, 321, 330.
RAMDAS, A. K. (1952). *Proc. Indian Acad. Sci.* A, **35**, 249; **36**, 55.
RAMDAS, L. A. (1926). *Indian J. Phys.* **8**, 231.
RAYLEIGH. (1888). *Phil. Mag.* (6), **26**, 241, 256.
RAYLEIGH. (1889). *Proc. Roy. Inst.* **12**, 447.
SHANTAKUMARI, C. (1950). *Proc. Indian Acad. Sci.* A, **32**, 177.
SIRKAR, S. C. (1930). *Indian J. Phys.* **5**, 337.
STOKES, G. G. (1885). *Proc. Roy. Soc.* **38**, 175.
WOOD, R. W. (1906). *Phil. Mag.* (6), **12**, 17.
ZACHARIASEN, W. H. (1929). *Z. Kristallogr.* **71**, 501.

Acta Cryst. (1957). **10**, 287

Neue Methoden zur Eliminierung des Spalteinflusses von röntgenographischen Kleinwinkelaufnahmen

VON VOLKMAR GEROLD

Institut für Metallphysik am Max-Planck-Institut für Metallforschung, Stuttgart, Deutschland

(*Eingegangen am* 14. *August* 1956)

In small-angle scattering measurements the use of a long slit rather than a pinhole for the definition of the incident beam implies a distortion of the measured angular intensity distribution $\bar{I}(x)$, from which the true intensity $I(r)$ (for an infinitely small pinhole) can be obtained as

$$I(r) = -\frac{1}{\pi}\int_r^\infty \frac{\bar{I}'(x)}{x}\frac{x}{\sqrt{(x^2-r^2)}}\,dx\,.$$

In the first part of the paper a simple instrument is described for quickly and accurately performing this reduction graphically. In the second part it is shown how the same instrument can be used for the same purpose if a slit of finite length limits either the incident or the diffracted beam.

1. Ein Gerät zur graphischen Korrektion des Spalteinflusses

Bei Kleinwinkelaufnahmen, die eine rotationssymmetrische Intensitätsverteilung $I(r)$ um einen Primärstrahl mit punktförmigem Querschnitt besitzen würden, verwendet man häufig zur Abkürzung der Belichtungszeit einen spaltförmigen Primärstrahl, so beispielsweise bei der neuen Streukammer von Kratky (1954, 1955). Man misst dann auf der Äquatorlinie eine Intensitätsverteilung $\bar{I}(x)$, die nicht mehr mit der gesuchten Verteilung $I(r)$ identisch ist, sondern infolge des entstehenden Kollimationsfehlers eine Verzerrung aufweist. Ist die Längsausdehnung des Primärstrahles mehr als das Doppelte des Streubereichs der Kleinwinkelstreuung, so kann man nach der Methode von Guinier & Fournet (1947) die gesuchte Kurve $I(r)$ aus der ersten Ableitung der experimentellen Kurve $\bar{I}'(x)$ erhalten. Es gilt die Beziehung

$$I(r) = -\frac{1}{\pi}\int_0^\infty \frac{\bar{I}'(\sqrt{(r^2+s^2)})}{\sqrt{(r^2+s^2)}}\,ds\,. \qquad (1)$$

Man geht praktisch so vor, dass man zunächst die Funktion $\varphi(x) = \bar{I}'(x)/x$ ermittelt. Diese wird dann für jeden r-Wert, für den man $I(r)$ berechnen will, im verzerrten Massstab $\varphi(\sqrt{(r^2+s^2)})$ als Funktion von s aufgetragen und entsprechend Gleichung (1) graphisch integriert. Dieses Verfahren ist sehr umständlich, da man beispielsweise für 20 Messpunkte 20 Kurven zeichnen und planimetrieren muss. Viel besser wäre es, wenn man für alle Integrationen nur eine einzige Kurve $\varphi(x)$ benötigen würde. Diese eine Kurve könnte dann als Schablone ausgebildet werden, wodurch die Planimetrierung wesentlich rascher und genauer vonstatten geht.

Formen wir Gleichung (1) durch die Abzissentransformation

$$x^2 = r^2+s^2 \qquad (2)$$

um, so erhalten wir:

$$I(r) = -\frac{1}{\pi}\int_r^\infty \varphi(x)\cdot\frac{x}{\sqrt{(x^2-r^2)}}\,dx\,. \qquad (3)$$

Wir benötigen nun ein Gerät, bei dem ein Fahrstift